

1 **Title: Motor skill learning leads to the increase of planning horizon**

2

3 **Authors**

4 Luke Bashford^{1,2,3,+,*}, Dmitry Kobak^{1,2,3,4++,*}, Jörn Diedrichsen⁵, Carsten Mehring^{1,2,3}

5

6 ¹Bernstein Center Freiburg, University of Freiburg, Freiburg, Germany

7 ²Faculty of Biology, University of Freiburg, Freiburg, Germany

8 ³Imperial College London, London, UK

9 ⁴Champalimaud Centre for the Unknown, Lisbon, Portugal

10 ⁵Brain and Mind Institute & Department for Computer Science, University of Western Ontario,

11 Ontario, Canada

12 ⁺Now at: Caltech, Pasadena, CA, USA

13 ⁺⁺Now at: Institute for Ophthalmic Research, Tübingen University, Tübingen, Germany

14 ^{*}Equal contribution

15

16 **Corresponding author**

17 Luke Bashford, bashford@caltech.edu

18 **Abstract**

19

20 We investigated motor skill learning using a path tracking task, where human subjects had to
21 track various curved paths at a constant speed while maintaining the cursor within the path
22 width. Subjects' accuracy increased with practice, even when tracking novel untrained paths.
23 Using a “searchlight” paradigm, where only a short segment of the path ahead of the cursor
24 was shown, we found that subjects with a higher tracking skill took a longer section of the
25 future path into account when performing the task. An optimal control model with a fixed
26 horizon (receding horizon control) that increases with tracking skill quantitatively captured the
27 subjects' movement behaviour. These findings demonstrate that human subjects increase their
28 planning horizon when acquiring a motor skill.

29 **Introduction**

30

31 The human motor system is able to acquire a remarkable array of motor skills.
32 Informally, a person is said to be “skilled” if he or she is able to perform faster and at the same
33 time more accurate movements than other, unskilled, individuals. What we don't know,
34 however, is what learning processes and components underlie our ability to move better and
35 faster. One component may be relatively “cognitive”, involving the faster and more
36 appropriate selection and planning of upcoming actions (Diedrichsen and Kornysheva, 2015;
37 Wong et al., 2015). Another component may be related to motor execution – the ability to
38 produce and fine control difficult combinations of muscle activations (Shmuelof et al., 2012;
39 Waters-Metenier et al., 2014). Depending on the structure of the task, changes in visuo-motor
40 processing or feedback control may also contribute to skill development. Motor adaptation,
41 extensively studied using visuomotor and force perturbations [for a recent review see
42 (Shadmehr et al., 2010)], may play a certain role in stabilizing performance, but it can not by
43 itself lead to improvements in the speed-accuracy trade-off (Wolpert et al., 2011).

44 A task commonly used in the experiments on motor skill learning is sequential
45 finger tapping, where subjects are asked to repeat a certain tapping sequence as fast and as
46 accurately as possible (Karni et al., 1998, 1995; Petersen et al., 1998; Walker et al., 2002).
47 Improvement in such a task can continue over days, but previous papers have focussed mostly
48 on the learning that is specific to the trained sequence(s) (Karni et al., 1995).

49 Many real-world tasks, however, do not involve the production of a fixed
50 sequence of motor commands, but the flexible planning and execution of movements. Such
51 flexibility is often well described by optimal feedback control models (Braun et al., 2009;
52 Diedrichsen et al., 2010; Todorov and Jordan, 2002) where the skilled actor appears to

53 compute “on the fly” the most appropriate motor command for the task at hand. This requires
54 demanding computations (Todorov and Jordan, 2002), and the human motor system likely
55 has found heuristics to deal with this complexity. One way to reduce complexity of the
56 control problem is to not optimize the whole sequence of motor commands that will achieve
57 the ultimate goal, but to only optimise the current motor command for a short distance into
58 the future. This idea is called receding horizon control, also known as model predictive
59 control (Kwon and Han, 2005). Under this control regime, the system computes a feedback
60 control policy that is optimal for a finite planning horizon. The control policy is then
61 continuously updated as the movement goes on and the planning horizon is being shifted
62 forward. This allows for adaptability, e.g. it can flexibly react to perturbations or unexpected
63 challenges, as sensory information becomes available. Recent studies provided indirect
64 evidence that favour the optimisation of short time-periods of a motor command (Dimitriou
65 et al., 2013). The notion of planning horizon also arises in reinforcement learning, e.g. in the
66 context of the so-called successor representation (Momennejad et al. 2017).

67 Motivated by these ideas, we propose that some of the skill of a down-hill skier or
68 a race-car driver may lie not only in the ability to execute difficult motor commands, but also
69 in the ability to plan further ahead and to optimize the movements for a longer time period into
70 the future. In addition, we propose that the time span that subjects plan ahead increases with
71 experience, leading to an increasing performance with training.

72 To test this idea, we designed an experimental condition which would allow us to
73 measure the planning horizon that skilled actors are using when executing long sequence of
74 movements that need to be planned “on the fly” – i.e. where the actual sequence of movements
75 cannot be memorized. For this, we developed a path tracking task, where subjects had to
76 maintain their cursor within a path that was moving towards them at a fixed speed. A similar
77 task has been previously used in motor control research (Poulton, 1974), using a mechanical

78 apparatus with paths drawn on a paper roll that was moving at a fixed speed. It has been shown
79 that subjects are able to increase their accuracy with training, but the different computational
80 strategies between expert subjects and naïve performers remain unclear. In our study we use
81 ‘searchlight’ trials in which subjects see various lengths of the approaching path ahead of their
82 cursor to probe subjects forward planning and compare experts and novices in this respect.

83

84 **Materials and Methods**

85 **Subjects**

86 62 experimentally naïve subjects took part in this experiment (33 males and 29 females, age
87 range 20-52 years old). Subjects gave informed consent and were paid 10 €/h. The experimental
88 procedures received ethics approval from the University of Freiburg.

89

90 **Setup**

91 Subjects sat at a desk looking at a computer monitor (Samsung Syncmaster 226BW) located
92 ~80cm away. A cursor displayed on the screen (Matlab and Psychophysics Toolbox Version
93 3; Brainard, 1997) was under position control by movements of a computer mouse. The mouse
94 could be moved on the desk in all directions but only the horizontal (left and right) component
95 contributed to the cursor movement: the vertical position of the cursor was fixed at 5.7mm
96 above the base of the screen.

97

98 **Task**

99 To begin each trial subjects had to press the space bar. This displayed the cursor ($R=2.9\text{mm}$,
100 1.1cm from the bottom of the screen) and the path (width = 2.83cm) that extended from the top

101 to bottom of the screen (30cm). The path continuously moved downward on the screen at a
102 vertical speed of 34.1cm/s. The initially visible path was a straight line centered in the middle
103 of the screen with the cursor positioned in the middle of the path. Once this initial section
104 moved through the screen, the path then followed a random curvature (Fig. 1A). Subjects were
105 instructed to keep the cursor between the path borders at all times moving only in the horizontal
106 plane and were told to be as accurate as possible. The cursor and path were displayed in white
107 if the cursor was within the path and both turned red when it was outside the path, always on a
108 black background.

109
110 The cursor position was sampled at 60 Hz and the tracking accuracy was defined for each trial
111 as the percentage of time steps when the cursor was inside the path. Running accuracy values
112 were continuously displayed in the top left corner of the screen and final accuracies were
113 displayed between the trials.

114
115 This experiment is based on a previous version where subjects were asked to track static
116 randomly curved paths in 2D as quickly as possible without touching the sides [unpublished
117 data, (Bashford et al., 2015)]. We later found that the 1D paradigm presented here was better
118 suited to study the planning horizon as the speed was fixed.

119 **Paradigm**

120 Subjects were randomly assigned into two groups: expert (N=32) and naive (N=30). The
121 paradigm included a training (expert group only) and a testing (all subjects) phase. Subjects in
122 the expert group trained over 5 consecutive days, each day completing 30 minutes of path
123 tracking (10 of 3-minute trials with short breaks in-between, searchlight length (s) 100%). If
124 the performance improved from one trial to the next subjects saw a message saying
125 “Congratulations! You got better! Keep it up!”, otherwise the message “You were worse this

126 time! Try to beat your score!” was shown. The training paths were randomly generated on the
127 fly. Experts performed the testing set of trials after a short break following training on the final
128 (5th) day. Naïve subjects performed only the testing set of trials.

129

130 The testing phase lasted 30 min (30 of 1-minute trials with breaks in-between) using 30
131 different pre-generated paths that were the same for all subjects. The testing phase in this
132 experiment contained 3 normal trials ($s=100\%$) and 27 searchlight trials ($s=10-90\%$) where
133 some upper part of the path was not visible. Three blocks of 10 trials with the searchlight length
134 ranging from $s=10\%$ to $s=100\%$ (in steps of 10%) were presented, with the order shuffled in
135 each block; the same fixed pseudorandom sequence was used for all subjects.

136

137 **Path generation**

138 Paths were generated before each trial start during training and a pre-generated fixed set was
139 produced in the same way for testing. Each path was initialized to start at the bottom middle of
140 the screen and the initial 30 cm of each path were following a straight vertical line. Subsequent
141 points of the path midline had a fixed Y step of 40 pixels (1.1 cm) and random independent
142 and identically distributed (iid) X steps drawn from a uniform distribution from 1 to 80 pixels
143 (2.7mm – 2.2cm). Any step that would cause the path to go beyond the right or left screen
144 edges was recalculated. The midline was then smoothed with a Savitzky-Golay filter (12th
145 order, window size 41) and used to display path boundaries throughout the trial. All of the
146 above parameters were determined in pilot experiments to create paths which were very hard
147 but not impossible to complete after training.

148

149 **Statistical analysis**

150 In all cases, we used nonparametric rank-based statistical tests to avoid relying on the normality
151 assumption. In particular, we used Spearman's correlation coefficient instead of the Pearson's
152 coefficient, Wilcoxon signed-rank test instead of paired two-sample t-test, and Wilcoxon-
153 Mann-Whitney ranksum test instead of unpaired two-sample t-test.

154

155 We initially recorded N=10 subjects in each group and observed statistically significant
156 ($p < 0.05$) effect that we are reporting here: positive correlation between the asymptote
157 performance and the horizon length, as estimated via the changepoint and exponential models.
158 We then recorded another N=20/22 (naïve/expert) subjects per group to confirm this finding.
159 This internal replication confirmed the effect ($p < 0.05$). The final analysis reported in this study
160 was based on all N=62 subjects together.

161

162 **Changepoint and Exponential model**

163 We used two alternative models to describe the relationship between the searchlight length and
164 the accuracy: a linear changepoint model and an exponential model. We used two different
165 models to increase the robustness of our analysis and both models support our conclusions.

166

167 The changepoint model is defined by

$$168 \quad y = \begin{cases} cs + o & \text{if } s \leq h_{cp} \\ ch_{cp} + o & \text{if } s > h_{cp} \end{cases}$$

169 where y is the subject's performance, s the searchlight length and (c, o, h_{cp}) are the subject-
170 specific parameters of the model which define the baseline performance at searchlight 0% (o),

171 the amount of increase of performance with increasing searchlight (c) and the planning horizon
172 (h_{cp}) after which the performance does not increase any further.

173

174 The exponential model is defined by

$$175 \quad y = \psi - \exp(-\rho s + d)$$

176 where the subject-specific parameters (ψ , d , ρ) specify the performance at searchlight 0% ($\psi -$
177 $\exp[d]$), the asymptote for large searchlights (ψ) and the speed of performance increase (ρ).

178 This function monotonically increases but it never plateaus. The speed of the increase depends
179 on the parameter ρ with larger values meaning faster approaching the asymptote. We used the
180 following quantity as a proxy for the “effective” planning horizon: $10 + \log(5)/\rho$. It can be
181 understood as the searchlight length that leads to performance being five times closer to the
182 asymptote than at $s=10\%$. The $\log(5)$ factor was chosen to yield horizon values of roughly the
183 same scale as with the changepoint model above.

184

185 Both models (changepoint and exponential) were fit to the raw performance data of each
186 subject, i.e. to the 30 data points, 3 for each of the 10 searchlight length values. The exponential
187 fit (see Equation 2 in the Results) was done with the Matlab's `nlinfit()` function, implementing
188 Levenberg-Marquardt nonlinear least squares algorithm. The changepoint fit (see Equation 1
189 in the Results) was done with a custom script that worked as follows. It tried all values of h_{cp}
190 on a grid that included $s=10\%$ and then went from $s=20\%$ to $s=100\%$ in 100 regular steps. For
191 each value of h_{cp} the other two parameters can be found via linear regression after replacing all
192 $s > h_{cp}$ values with h_{cp} . We then chose h_{cp} that led to the smallest squared error.

193

194 **Trajectory analysis**

195 To shed light on the learning process we analysed additional parameters of the subjects'
196 movement trajectories.

197 First, we computed the time lag between the subjects' movement trajectories and the midline
198 of the paths (Figure 4A-B). To compute the lags, we interpolated both cursor trajectories and
199 path midlines 10-fold (to increase the resolution of our lag estimates). We computed the
200 Pearson correlation coefficient between cursor trajectory and path midline for time shifts
201 from of -300 to 300 ms, and defined the time lag as the time shift maximizing the correlation.
202 Second, we extracted the cursor trajectories in all sections across all paths that shared a
203 similar curved shape to explore the differences in cursor position at the apex of the curve
204 (Figure 4C). The segments were selected automatically by sliding a window of length 18 cm
205 across the path. We included all segments that were lying entirely to one side (left or right) of
206 the point in the middle of the sliding window ("C-shaped" segments), with the upper part and
207 the lower part both going at least 4.5 cm away in the lateral direction (see Figure 3). Our
208 results were not sensitive to modifying the exact inclusion criteria.

209 To draw the 75% coverage areas of the path inflection points in each group (Figure 4C), we
210 first performed a kernel density estimate of these points using the Matlab function `kde2d()`,
211 which implements an adaptive algorithm suggested in (Botev et al., 2010). After obtaining the
212 2d probability density function $p(x)$, we found the largest h such that $\int p(x)dx > 0.75$ over the
213 area where $p(x) > h$. We then used Matlab's `contour()` function to draw contour lines of height h
214 in the $p(x)$ function.

215

216

217

218 Receding horizon model

219 We modelled subjects' behaviour by a stochastic receding horizon model in discrete time t . In
220 receding horizon control (RHC, Kwon and Han, 2005) motor commands u_t are computed to
221 minimize a cost function L_t over a finite time horizon of length h :

$$222 \quad \text{minimize } L_t(\{x_t\}, \{u_t\}) \quad (1)$$

$$223 \quad \text{subject to } L_t = \sum_{k=1}^h l_{t+k}$$

$$224 \quad x_{t+1} = f(x_t, u_t)$$

225 where f defines the dynamics of the controlled system. Equation (1) is equivalent to an optimal
226 control problem over the fixed future interval $[t + 1, t + h]$. Solving (1) yields a sequence of
227 optimal motor commands $\{u_0^{opt}, u_1^{opt}, \dots, u_{h-1}^{opt}\}$. The control applied at time t is the first
228 element of this sequence, i.e. $u_t = u_0^{opt}$. Then, the new state of the system x_{t+1} is measured
229 (or estimated) and the above optimization procedure is repeated, this time over the future
230 interval $[t + 2, t + 1 + h]$, starting from the state x_{t+1} .

231

232 Applying RHC to our experimental task, the dynamics of the cursor movement was modelled
233 by a linear first-order difference equation:

$$234 \quad x_{t+1} = x_t + u_{t-\tau} + \eta_t \quad \eta_t \in \mathcal{N}(0, \sigma^2) \quad (2)$$

235 where t is the time step, x_t the cursor position at time t , u_t is the motor command applied at
236 time t and τ the motor delay. η_t is the motor noise which was modelled as additive Gaussian
237 white noise with zero mean and variance σ^2 . We used the following cost function

$$238 \quad L_t = \sum_{k=\tau+1}^h [-\log(q_{t+k}) + \lambda |u_{t-\tau+k-1}|^2] \quad (3)$$

239 where L_t is the expected cost at time t , q_{t+k} is the probability of the cursor being inside the path
 240 at time $t+k$, h is the length of the horizon in time and λ is the weight of the motor command
 241 penalty. At every time step t , L_t is minimized to compute u_t while $\{u_0, \dots, u_{t-1}\}$ are known.
 242 Consequently, the lower bound of the sum in (3) is $\tau + 1$. The cost function in (3) reflects a
 243 trade-off between accuracy (first term, i.e. $\log[q_{t+k}]$) and effort (second term) whereas their
 244 relative importance is controlled by λ . Cost functions with a similar accuracy-effort trade-off
 245 have been used previously to successfully model human motor behaviour (Todorov & Jordan
 246 2002, Diedrichsen 2007, Braun et al. 2009).

247 We assume that subjects have acquired a forward model of the control problem and they can,
 248 therefore, predict the cursor position at time $t+1$ from the cursor position at time t and the motor
 249 command in accordance with equation (2). We also assume that subjects have an accurate
 250 estimate of the position of the cursor at time t , i.e. x_t is known. Subjects can then compute the
 251 probability distribution of the cursor position at future times $t+k$, given by:

$$252 \quad p(x_{t+k} | x_t, \{u_{t-\tau}, u_{t-\tau+1}, \dots, u_{t-\tau+k-1}\}) = \frac{1}{\sqrt{2\pi k\sigma^2}} e^{-\frac{(\hat{x}_{t+k})^2}{2k\sigma^2}} \quad (5)$$

253 with

$$254 \quad \hat{x}_{t+i} = x_t + \sum_{l=1}^i u_{t-\tau+l-1} \quad (6)$$

255 The probability of the cursor being inside the path is then given by

$$256 \quad q_{t+k} = \int_{m_{t+k}-\frac{w}{2}}^{m_{t+k}+\frac{w}{2}} \frac{1}{\sqrt{2\pi k\sigma^2}} e^{-\frac{(\hat{x}_{t+k}-z)^2}{2k\sigma^2}} dz \quad (7)$$

257 where m_t is the position of the midline of the path at time t and w the width of the path. The
 258 receding horizon model assumes that motor commands u_t are computed by minimizing the
 259 cost L_t in each time step t for a fixed and known set of model parameters $(h, \lambda, \tau, \sigma^2)$. We
 260 simplify the optimisation problem by approximating q_{t+k} by

$$261 \quad q_{t+k} \approx w \frac{1}{\sqrt{2\pi k\sigma^2}} e^{-\frac{(\hat{x}_{t+k} - m_{t+k})^2}{2k\sigma^2}} \quad (8)$$

262 The higher $k\sigma_k^2$ is relative to the path width w , the higher the accuracy of this approximation.

263 Note that the squared error is scaled by $k\sigma^2$ and hence, errors in the future are discounted. This

264 is a consequence of the used model of the cursor dynamics in (equation 2).

265 Using equation (8) and removing all terms which do not depend on u_t , we can derive a

266 simplified cost function

$$267 \quad \tilde{L}_t = \sum_{k=\tau+1}^h \left[\frac{(\hat{x}_{t+k} - m_{t+k})^2}{2k\sigma^2} + \lambda |u_{t-\tau+k-1}|^2 \right] \quad (9)$$

268 Equation (9) shows that the trade-off between accuracy and the magnitude of the motor

269 commands is controlled by $\sigma^2\lambda$. We therefore can eliminate one parameter and use the

270 equivalent cost function

$$271 \quad \tilde{L}_t = \sum_{k=\tau+1}^h \left[\frac{(\hat{x}_{t+k} - m_{t+k})^2}{2k} + \tilde{\lambda} |u_{t-\tau+k-1}|^2 \right] \text{ with } \tilde{\lambda} = \sigma^2\lambda \quad (10)$$

272 The gradient of the cost function \tilde{L}_t is given by

$$273 \quad \frac{\partial \tilde{L}_t}{\partial u_{t+j}} = 2\tilde{\lambda} u_{t+j} + \sum_{k=j+(\tau+1)}^h \left[\frac{(\hat{x}_{t+k} - m_{t+k})}{k} \right] \quad (11)$$

274 with $j = 0, \dots, h - (\tau + 1)$. The Hessian of the cost function is given by

$$275 \quad \frac{\partial^2 \tilde{L}_t}{\partial u_{t+m} \partial u_{t+n}} = 2\delta_{m,n}\tilde{\lambda} + \sum_{k=\max(m,n)+(\tau+1)}^h \frac{1}{k} \quad (12)$$

276 with $m, n = 0, \dots, h - (\tau + 1)$. For $\tilde{\lambda} = 0$ all pivots of the Hessian matrix are positive and

277 therefore the Hessian is positive definite for $\tilde{\lambda} = 0$. For the general case $\tilde{\lambda} > 0$ the Hessian

278 remains positive definite as $H_2 = H_1 + D$ is positive definite if H_1 is positive definite and D is

279 a diagonal matrix with only positive diagonal entries. Given the positive definiteness of the

280 Hessian we can conclude that the cost function \tilde{L}_t is strictly convex with a unique global

281 minimum. Setting the gradient (12) to $\mathbf{0}$ defines a system of $h-\tau$ linear equations with $h-\tau$
 282 unknowns $(u_t, \dots, u_{t+h-(\tau+1)})$ which solution minimizes \tilde{L}_t . The solution can be computed
 283 efficiently using standard numerical techniques. We used the ‘linsolve’ function of MATLAB
 284 (R2016b) which uses LU factorization.

285 As a measure of task performance, we computed the expected time inside the path from the
 286 model trajectory z_t as follows

$$290 \quad a = \frac{1}{T} \sum_{t=1}^T \left[1 - \int_{m_{t-\frac{w}{2}}}^{m_{t+\frac{w}{2}}} \frac{1}{\sqrt{2\pi\sigma^2}} e^{-\frac{(z_t-\eta)^2}{2\sigma^2}} d\eta \right] \quad (13)$$

287 with T depicting the number of time steps per path. The lag was computed by maximizing the
 288 correlation coefficient between the model trajectories and the path midline identical to how the
 289 lag was computed for the subjects’ trajectories.

291 When applying the model to the searchlight path we made the additional assumption that the
 292 model horizon increases with searchlight length s up to a maximal value h_{max} beyond which
 293 the model horizon remains constant:

$$295 \quad h(s) = \begin{cases} s, & s < h_{max} \\ h_{max}, & s \geq h_{max} \end{cases} \quad (14)$$

294

296 **Fitting the receding horizon model to subjects’ behaviour**

297 We fitted the RHC model to the subjects’ movement trajectories in the searchlight testing paths
 298 using Bayesian inference (Gelman et al. 2000). The model parameters were estimated by
 299 computing their expected values from the posterior distribution

$$300 \quad \hat{\beta} = \langle \beta \rangle = \int \beta p(\beta|v) d\beta \quad (15)$$

301 where β is the model parameter, v the movement trajectory data of a subject and $p(\beta|v)$ the
 302 posterior probability distribution for β . We approximated the integral in (15) by sampling from
 303 the posterior distribution using the Metropolis algorithm which can sample from a target

304 distribution that can be computed up to a normalizing constant (Gelman et al. 2000). The RHC
 305 model has four parameters $(h_{max}, \tau, \tilde{\lambda}, \sigma^2)$ out of which three $(h_{max}, \tau, \tilde{\lambda})$ affect the shape of
 306 the trajectory (cf. equation (10)). Assuming a flat prior for the model parameters, i.e. .
 307 $p(h_{max}, \tau, \tilde{\lambda}) = \text{const.}$, and a non-informative prior for the error-variance δ^2 , i.e. $p(\delta^2) = 1/\delta^2$
 308 (Gelman et al 2000), we obtained the following equation for the posterior

$$312 \quad p(\beta|w) \propto p(h_{max}, \tau, \tilde{\lambda}) \frac{1}{\delta^{2+N}} e^{-\frac{mse(h_{max}, \tau, \tilde{\lambda})}{2\delta^2}} \quad (16)$$

309 where $mse(h_{max}, \tau, \tilde{\lambda})$ is the mean squared error between the model and the subject movement
 310 trajectories and N the number of trials. The mean squared error between the movement
 311 trajectories of a subject and the model is given by

$$313 \quad mse(h_{max}, \tau, \tilde{\lambda}) = \frac{1}{10T|\mathcal{F}|} \sum_{s=1}^{10} \sum_{j \in \mathcal{F}_s} \sum_{t=1}^T \left(v_t^{(s,j)} - z_t^{(s,j)}(h_{max}, \tau, \tilde{\lambda}) \right)^2 \quad (17)$$

314 with T depicting the number of time steps per path, \mathcal{F}_s the set of paths ids for searchlight s ,
 315 $v_t^{(s,j)}$ the movement of subject i at time t in path j for searchlight s and $z_t^{(s,j)}(h_{max}, \tau, \tilde{\lambda})$ the
 316 corresponding movement predicted by the RHC model.

317 To save computation time, we precomputed the mse for specific discrete combinations of the
 318 model parameters. The model horizon parameter h_{max} could take any integer value between 1
 319 and 26 given a maximum possible planning horizon of 30cm (vertical screen size) which is
 320 equivalent to $30\text{cm} / \left(34 \frac{\text{cm}}{\text{s}} \cdot \frac{1}{30} \text{s} \right) = 30\text{cm} / \left(\frac{34}{30} \text{cm} \right) \approx 26$ time steps, where 34 cm/s is the
 321 path speed and 1/30s the time step. Hence, admissible values for the horizon parameter
 322 corresponded to horizons of $h_{max} = (1, \dots, 26) * \frac{34}{30} \text{cm}$. For the delay we allowed the values
 323 $\tau = (1, \dots, 15) * \frac{1}{30} \text{s}$, assuming that subjects won't have larger delays than 500ms. In fact, the
 324 maximum delay of a subject we found from fitting was 286 ms which is well below the limit
 325 we imposed. The motor penalty parameter $\tilde{\lambda}$ was allowed to take any of 10^3 logarithmically

326 equally spaced values between 10^{-4} and 10^7 and 0. In total, we had, therefore,
327 $26 \times 15 \times 1001 = 390390$ admissible parameter combinations for h_{max} , τ and $\tilde{\lambda}$. We simulated the
328 model for all of these parameter values and computed the mean squared errors according to
329 equation (17). We then used the Metropolis algorithm to generate 10^6 samples from the
330 posterior distribution of the parameters. Each sample consisted of a 4-tuple of values for the
331 parameters $(h_{max}, \tau, \tilde{\lambda}, \delta^2)$. We computed the motor noise parameter of the model σ^2 from the
332 estimated error-variance δ^2 as explained below and then $\lambda = \tilde{\lambda}/\sigma^2$ (cf. equation 10). For each
333 parameter sample we also computed the lag, as explained at the end of the previous section,
334 and the task performance using equation (13). As a result, we obtained 10^6 parameter values,
335 lags and task performances, which reflect samples from the posterior distribution of the model
336 parameters.

337 To evaluate the quality of the model, we used three-fold cross-validation where in each fold
338 the posterior distributions of the model parameters were estimated using the data from two of
339 the three trials for each searchlight. The posterior distributions were then used to make model
340 predictions of performance and lag in the remaining trial for each searchlight. This was done
341 for each subject separately and the model predictions were compared to the experimentally
342 observed performances and lags (cf. Fig. 5A-D).

343 Expected values of the model parameters were computed according to equation (13). Expected
344 values were calculated for each cross-validation fold separately and then averaged across the
345 three cross-validation folds. This yielded the model parameters $h_{max}, \tau, \lambda, \sigma^2$ for each subject,
346 shown in Fig. 5E-H.

347

348 *Estimation of the motor noise parameter from the error-variance*

349 If all model assumptions are fulfilled, the motor noise model parameter σ^2 will be linearly
350 related to the error-variance δ^2 and we should therefore be able to estimate σ^2 from δ^2 . For

351 each subject we computed σ^2 by minimizing the squared error between the model task
352 performance (eq. 13) and the experimentally determined task performance. A scatter plot of
353 the resulting σ^2 over the error-variance δ^2 revealed an approximate linear relationship between
354 σ^2 and δ^2 . We then determined the proportionality factor α by linear-least squares regression
355 of the model $\sigma^2 = \alpha\delta^2$ and used it to compute σ^2 from δ^2 . The linear-least squares regression
356 was done for each subject separately, using only the σ^2 and δ^2 values from all other subjects
357 to avoid overfitting.

358

359 **Estimating the influence of model parameters on performance difference between expert** 360 **and naïve groups**

361 To estimate how much a single model parameter causes the experts' gain in performance we
362 computed the performance of the model for naïve group parameters but with one parameter
363 (horizon, motor noise, delay or motor penalty) changed to expert group values. We also
364 performed the opposite procedure, replacing each parameter for each participants of the expert
365 with those of the naïve group. Using the Bayesian inference approach described in the previous
366 section, we replaced the full posterior distribution of the affected parameter with the posterior
367 distribution from the other group. This procedure was carried out for each subject separately
368 and the posterior of the affected parameter was replaced by the posterior of each subject from
369 the other group separately. We then computed the posterior of the performance curve and from
370 that the expected values of the performance by averaging. Hence, we obtained for each
371 parameter change $N_e \cdot N_n$ performance curves where N_e and N_n are the number of subjects in
372 the expert and naïve group, respectively. These performance curves were averaged and
373 compared to the average performances for the expert and naïve groups obtained for the fitted
374 model (see Results for details).

375

376 Parts of the modelling computations were run on the high-performance computing cluster

377 NEMO of the University of Freiburg (<http://nemo.uni-freiburg.de>) using Broadwell E5-2630v4

378 2.2 GHz CPUs.

379

380 Results

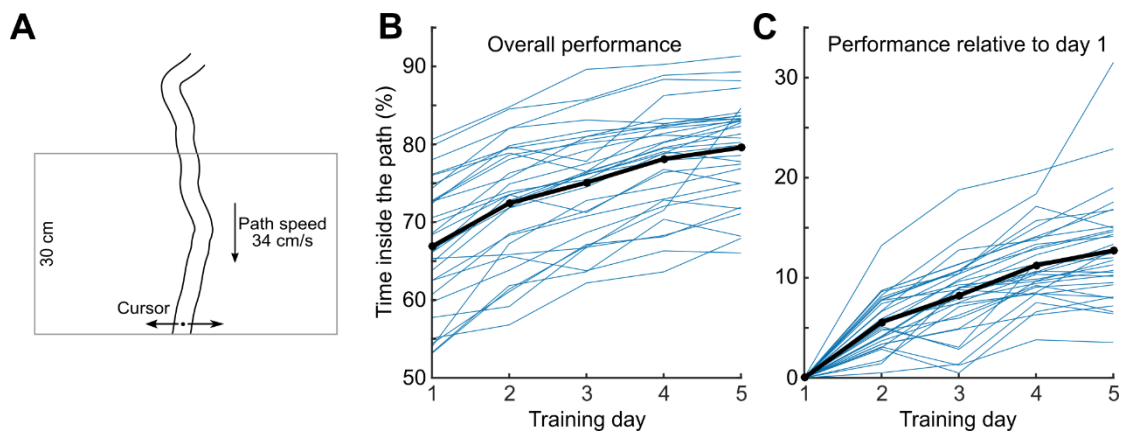
381

382 Learning the Tracking Skill

383 We designed an experiment where subjects had to track a path moving towards them at a
384 fixed speed (Fig. 1A and Methods). The narrow and wiggly path was moving downwards on a
385 computer screen while the cursor had a fixed vertical position in the bottom of the screen and
386 could only be moved left or right. Accuracy, our performance measure, was defined as the
387 fraction of time that the cursor spent inside the path boundaries. One group of subjects (the
388 expert group, N=32) trained this task for 30 minutes on each of 5 consecutive days. Another
389 group (the naïve group, N=30) did not have any training at all. Both groups then performed a
390 testing block that we describe below.

391

392



393

394 *Figure 1. Experimental Paradigm. (A) Subjects had to track a curved path that was dropping*
395 *down from top to bottom of the screen with a fixed speed of 34 cm/sec by moving the cursor*
396 *horizontally. (B) Expert subjects' performance over the 5 days of training. Bold line shows the*
397 *group average, thin lines show individual subjects (each point is a mean over 3 trials with the*

398 *same searchlight length, 100%). (C) Expert subjects' performance over the 5 days of training*
399 *with the performance on the first day subtracted.*

400

401

402 Over the course of five training days, the experts' accuracy increased from $66.9 \pm 8.0\%$ to
403 $79.6 \pm 6.4\%$ (mean \pm SD across subjects, first and last training day respectively) as shown on Figs
404 1B-C, with the difference being easily noticeable and statistically significant ($p = 8 \cdot 10^{-7}$,
405 $z = 4.9$, Wilcoxon signed rank test; Cohen's $d = 1.8$, $N = 32$). As all paths generated during the
406 training were different, this difference cannot be ascribed to memorizing the path, therefore
407 this improvement represents the genuine acquisition of the skill of path tracking.

408

409 **Searchlight testing**

410 To unravel the mechanisms of skill acquisition we designed testing trials called “searchlight
411 trials”, during which subjects had to track curved paths as usual, but could only see a certain
412 part of the path (fixed distance s) ahead of the cursor. The searchlight length s varied between
413 10% and 100% of the whole path length in steps of 10% (the minimal s was ~ 3 cm) to probe
414 subjects' planning horizon. During the testing block all subjects completed 30 one-minute-long
415 trials (three repetitions of each of the 10 values of s). The average accuracy at full searchlight
416 $s = 100\%$ was $82.8 \pm 7.5\%$ for the expert group and $65.7 \pm 8.4\%$ for the naïve group (mean \pm SD
417 across subjects), with the difference being highly significant ($p = 2 \cdot 10^{-9}$, $z = 6.0$, Wilcoxon-
418 Mann-Whitney ranksum test, Cohen's $d = 2.2$, $N = 62$). The performance of the naïve subjects
419 matched the initial performance of the expert subjects on their first day of training.

420

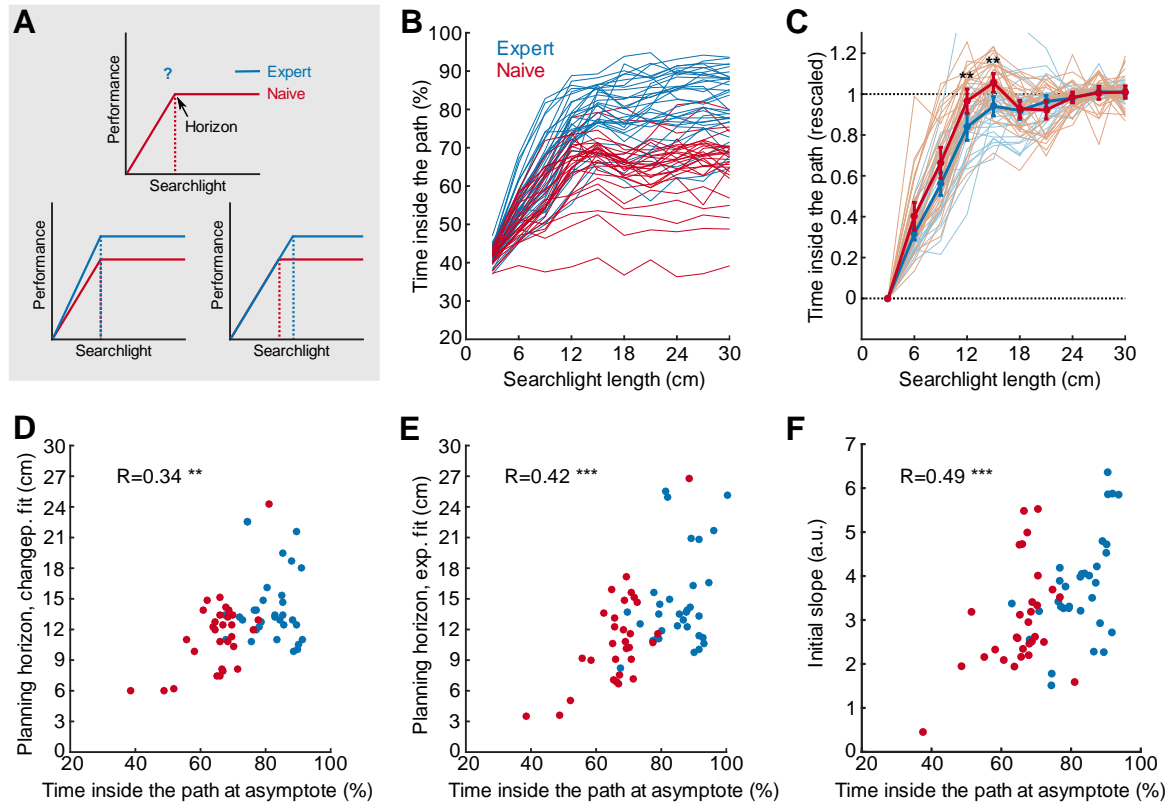
421 Before we present the rest of the data, let us consider several potential outcomes for the
422 dependence of accuracy on the searchlight length (Fig. 2A). It is clear that for each subject,
423 accuracy should be a non-decreasing function of searchlight length. The data presented in
424 Poulton (1974) indicate that this function tends to become flat, i.e. subjects reach a performance
425 plateau, after a certain value of searchlight length that we will call *planning horizon* (Fig. 2A
426 Top), while we assume all subjects will be constrained to the similar poor performance at the
427 smallest searchlight. For the expert group, this function has to reach a higher point at $s=100\%$,
428 but it could do so because the initial rise becomes steeper (Fig. 2A bottom left), or because the
429 planning horizon increases (Fig. 2A bottom right), or possibly both.

430

431 Fig. 2B shows subjects' accuracy in the searchlights trials as a function of the searchlight length
432 s . It is obvious that all subjects were strongly handicapped at short searchlights, and at the
433 shortest searchlight the performance of the two groups was similar with experts being only
434 marginally better ($42.5\pm 2.3\%$ for the expert group, $41.4\pm 1.8\%$ for the naïve group, $p=0.042$,
435 $z=2.0$ Wilcoxon ranksum test; Cohen's $d=0.5$, $N=62$).

436

437



438

439

440 *Figure 2. Searchlight testing. (A) Expert subjects were trained to have a higher performance*
 441 *at full searchlight length (top). This could be achieved by an increased initial slope (bottom*
 442 *left) at smaller searchlight length and/or an increased planning horizon as indicated with*
 443 *dashed vertical lines (bottom right). (B) Mean tracking performance for each searchlight*
 444 *length for each individual subject, in blue for the expert group and in red for the naïve group.*
 445 *Faint lines show individual subjects and bold lines show group means. (C) Mean tracking*
 446 *performance for each searchlight length, rescaled for each subject to start at 0 and end at 1*
 447 *(see text). Error bars indicate 95% confidence intervals around the means, stars indicate*
 448 *significance between the groups (**: $p < 0.01$, Wilcoxon rank sum test, Bonferroni-Holm*
 449 *corrected for multiple comparisons). (D-E) Planning horizon for each subject was defined by*
 450 *fitting a changepoint linear-constant curve (D) or an exponential curve (E) (see text). Both*
 451 *models yield an asymptote performance for each subject; the changepoint model yields a*

452 horizon length and the exponential fit yields an “effective” horizon length. The scatter plots
453 show relation between the asymptote performance (as a proxy for subjects' skill) and their
454 planning horizon. Spearman's correlation coefficients are shown on the plot (**: $p < 0.01$, ***:
455 $p < 0.001$). Colour of the dot indicates the group. (F) Scatter plot showing Spearman correlation
456 coefficient between the planning horizon and initial slope of the curve (10-20% in A), colours
457 and values as in D&E (***: $p < 0.001$).

458

459

460 Visual inspection of Fig. 2B suggests that both effects sketched in Fig. 2A contribute to expert
461 performance. (i) the planning horizon for the expert group was longer than for the naïve group;
462 and (ii) the expert group has higher accuracies in the initial part of the performance curve,
463 before the performance plateaus.

464

465 To better visualize the change in performance across searchlight lengths, we linearly rescaled
466 each subject's performance curve, first by subtracting the mean performance at $s=10\%$ and then
467 by dividing by the asymptote performance (computed as the mean performance across $s=80\%$ -
468 100%). The resulting curves all start at 0 and end at 1 (Fig. 2C). We observed a significant
469 difference between the groups at $s=40\%$ & 50% ($p=0.005$ and $p=0.004$ respectively, Wilcoxon
470 ranksum test, p -values adjusted for testing 6 searchlight lengths between 20% and 70% with
471 Holm-Bonferroni procedure, $N=62$), indicating that while naïve subjects had reached their
472 plateau by then, the expert subjects kept increasing their performance. For this analysis we
473 removed two naïve subjects with essentially flat searchlight curves (Fig. 1B), as rescaling those
474 did not lead to meaningful results.

475

476 To investigate individual differences in tracking skill, we estimated the planning horizons of
477 individual subjects (Fig. 2D). For this we fit each subject's performance (y) with a changepoint
478 linear-constant curve (see Methods), where the location of the changepoint defines the horizon
479 length. We found that the novice group had an average horizon length of 11.5 ± 3.6 cm
480 (mean \pm SD) and the expert group a horizon length of 14.2 ± 3.5 cm, with statistically significant
481 difference ($p=0.007$, $z=2.7$, Wilcoxon ranksum test; Cohen's $d=0.8$, $N=62$). We found a
482 positive correlation between the horizon length and the asymptotic performance ($R=0.34$,
483 $p=0.006$, Spearman correlation, $N=62$).

484

485 In addition to the change-point model, we also quantified the planning horizon using a single
486 exponential to fit the individual subjects' performance data (see Material and Methods). This
487 analysis confirmed our results (Fig. 2E). We again observed a significant difference in the
488 horizon length between the two groups (14.76 ± 4.6 cm vs. 11.04 ± 4.7 cm, means \pm SD for both
489 groups, $p=0.002$, $z=3.0$, Wilcoxon ranksum test; Cohen's $d=0.8$, $N=62$). Again, we found a
490 positive correlation between the asymptote performance and the effective horizon length
491 ($R=0.43$, $p=0.0008$, Spearman correlation, $N=62$).

492

493 Not only was planning horizon positively correlated with tracking skill (the asymptote
494 accuracy), but also the initial slope of the changepoint model. Fig. 2F shows the correlation
495 between the initial slope and asymptote accuracy ($R=0.49$, $p=6 \cdot 10^{-5}$, Spearman correlation,
496 $N=62$) and a clear difference of the initial slope between the groups ($p=0.008$, $z=2.6$, Wilcoxon
497 ranksum test; Cohen's $d=0.6$, $N=62$). We therefore conclude that the difference between expert
498 and naïve performances is a combination of both possibilities presented in Fig. 2A.

499

500

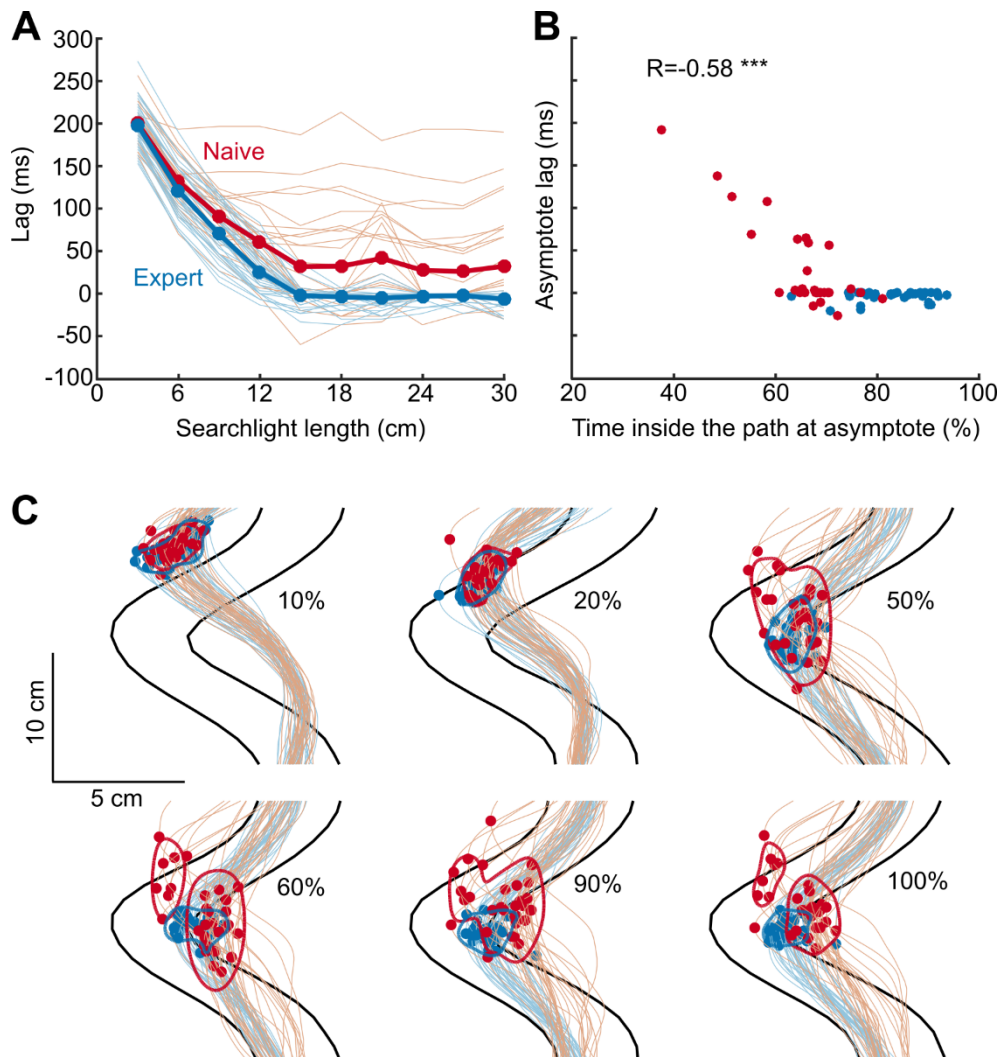
501 **Trajectory analysis**

502 Naïve subjects performed worse than the expert subjects at long searchlights but all subjects
503 performed almost equally badly at short searchlights. What kinematic features can these
504 differences be attributed to?

505

506 Clearly, at short searchlights, performance has to be reactive. To measure how quickly changes
507 in the path were reflected in the motor commands, we computed the time lag between cursor
508 trajectory and path midline (the lag maximizing cross-correlation between them). As Fig. 3A
509 shows the lag was ~200 ms at s=10% for all subjects and dropped to ~0 ms at s=50% for the
510 expert group. While many naïve subjects also decreased their lags to zero, 10 out of 30 never
511 achieved the 0 ms lag. The five naïve subjects showing the largest lags at large searchlights
512 were also those with the worst performance (Fig. 3B). Therefore, there was a strong negative
513 correlation between the asymptote lag (mean across s=80-100%) and the asymptote
514 performance (mean across s=80-100%) of $r=-0.58$ (Fig. 3B, $p=8 \cdot 10^{-7}$, Spearman correlation,
515 $N=62$).

516



517

518

519 *Figure 3. Analysis of trajectories. (A) Mean time lag between cursor trajectory and path*
520 *midline, for each searchlight length for each individual subject (faint lines) and mean of per-*
521 *subject values (bold lines), in blue for the expert group and in red for the naïve group. (B)*
522 *Asymptote lag and asymptote performance across subjects. Correlation coefficient is shown on*
523 *the plot (***) $p < 0.001$). Colour of the dot indicates the group. (C) Average per-subject*
524 *trajectories in sharp bends (leftward bends were flipped to align them with the rightward*
525 *bends). Each trajectory is averaged across approximately 40 bends (the number of bends*
526 *varied across searchlight lengths). Colour of the lines indicates the group. Black lines show*
527 *average path contour. Dots show turning points of the trajectory. Contour lines show the kernel*

528 *density estimate 75% coverage areas. Subplots correspond to searchlight lengths $s=10\%$, 20% ,*
529 *50%, 60%, 90% and 100%.*

530

531 Next, for each testing path we found all segments exhibiting sharp leftward or rightward bends
532 (see materials and methods, our inclusion criteria yielded 13 ± 5 segments per path, $\text{mean}\pm\text{SD}$).
533 For each searchlight length s and for each subject, we computed the average cursor trajectory
534 over all segments ($N=38\pm 8$ segments per searchlight) after aligning all segments on the bend
535 position (Fig. 3C, leftward bends were flipped to align them with the rightward bends). At
536 $s=10\%$ all subjects from both groups follow very similar lagged trajectories, resulting in low
537 accuracy. As searchlight increases, expert subjects reach zero lag and choose more and more
538 similar trajectories, whereas naïve subjects demonstrate a wide variety of trajectories with some
539 of them failing to reach zero lag and others failing to keep the average trajectory inside the path
540 boundaries. To visualize this, we plotted the kernel density estimate 75% coverage contour of
541 inflection points for each group. As the searchlight increases, the groups become less
542 overlapping and the naïve group appears to form a bimodal distribution (Fig. 3C).

543

544 In summary, at very short searchlights all subjects performed poorly because in this reactive
545 regime their trajectories lagged behind the path. At longer searchlights the expert subjects were
546 able to plan their movement to accommodate the bends (the longer the searchlight the better),
547 but naïve subjects failed to do so in various respects: either still lagging behind or not being
548 able to plan a good trajectory.

549

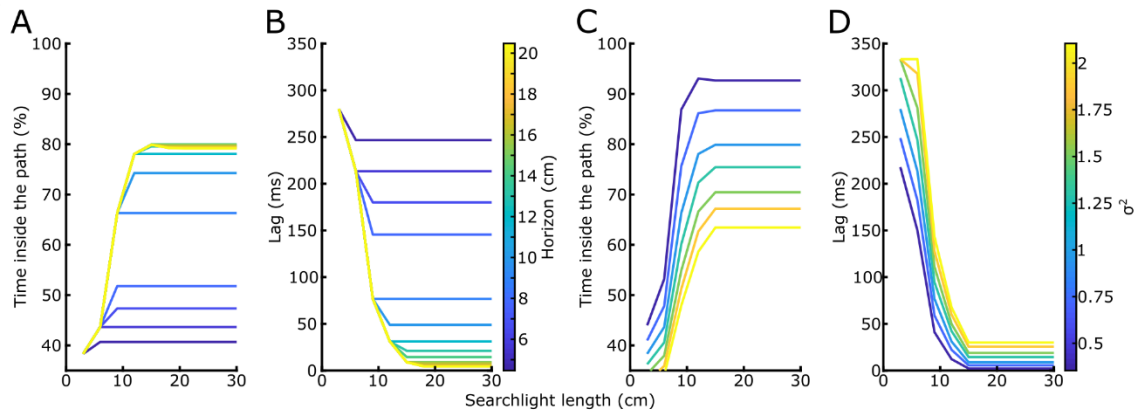
550 **Receding horizon model analysis**

551 Next, we modelled subjects' behaviour by receding horizon control (RHC). In RHC a sequence
552 of motor commands is computed to minimize the expected cost over a future time interval of

553 finite length, i.e. the horizon. After the first motor command is applied, the optimization
554 procedure is repeated using a time interval shifted one time step ahead. See Methods section
555 for a more detailed and formal description of RHC. As cost function, we used the weighted
556 sum of a measure of inaccuracy (i.e. probability of being outside the path) and the magnitude
557 of the motor cost (see Methods for details). Cost function with a similar trade-off between
558 movement accuracy and motor command magnitude have been used previously to describe
559 human motor behaviour in different tasks (Todorov & Jordan 2002, Diedrichsen 2007, Braun
560 et al. 2009). The model has four different parameters: horizon (h), motor noise (σ^2), motor
561 delay (τ) and motor command penalty weight (λ).

562 We ran the model on the experimental paths to obtain simulated movement trajectories from
563 which task performance and lag could be computed in the same way as for the experimental
564 trajectories (Fig. 2 and 3). Our simulations revealed that both, a larger model horizon as well
565 as a smaller motor noise parameter increased the task performance and decreased the lag (Fig.
566 4). Hence, the experimentally observed higher performance and smaller lag of expert subjects
567 compared to naive (Fig. 2B and 3A) could be explained either by an increased model horizon
568 or by reduced motor noise in the model. However, the searchlight length at which the task
569 performance of the model reached a plateau increased with model horizon and did not change
570 or even decreased with a smaller motor noise parameter (Fig. 4A, C). Experimentally, on the
571 other hand, we observed that subjects with a higher task performance reached their
572 performance plateau at higher searchlights (Fig. 2D, E). This correlation between performance
573 and plateau onset, that was observed experimentally, cannot be explained by the variation of
574 the motor noise parameter across subjects, but is only consistent with an increase of the model
575 planning horizon for subjects with higher performance.

576



577

578 *Figure 4: Task performance and lag as a function of searchlight length for model simulations*

579 *with different horizons (A,B) or different amounts of motor noise (C,D). A motor noise of $\sigma^2=1$*

580 *was used for (A,B) and a horizon of $h=15\text{cm}$ for (C,D). The motor delay and motor command*

581 *penalty weight were fixed at $\tau=200\text{ms}$ and $\lambda=0.5$ in all simulations.*

582

583 Next, we used Bayesian inference to estimate the model parameters from the experimentally

584 observed movement trajectories (see Methods for details). Based on inferred distributions of

585 parameter values, we then predicted task performance and lag for each subject. To avoid over-

586 fitting cross-validation was used, i.e. fitting and prediction was done on different trials. Model

587 task performance and lag resembled the experimentally observed task performance and lag

588 with regard to their change across searchlights as well as with regard to the difference between

589 naïve and the expert subjects (Fig. 5A,B). On a single subject and trial level there was a high

590 correlation between model and experimental task performance (Fig. 5C, Spearman correlation

591 $r=0.9$, $R^2=0.84$) and lags (Fig. 5D, Spearman correlation $r=0.87$, $R^2=0.88$).

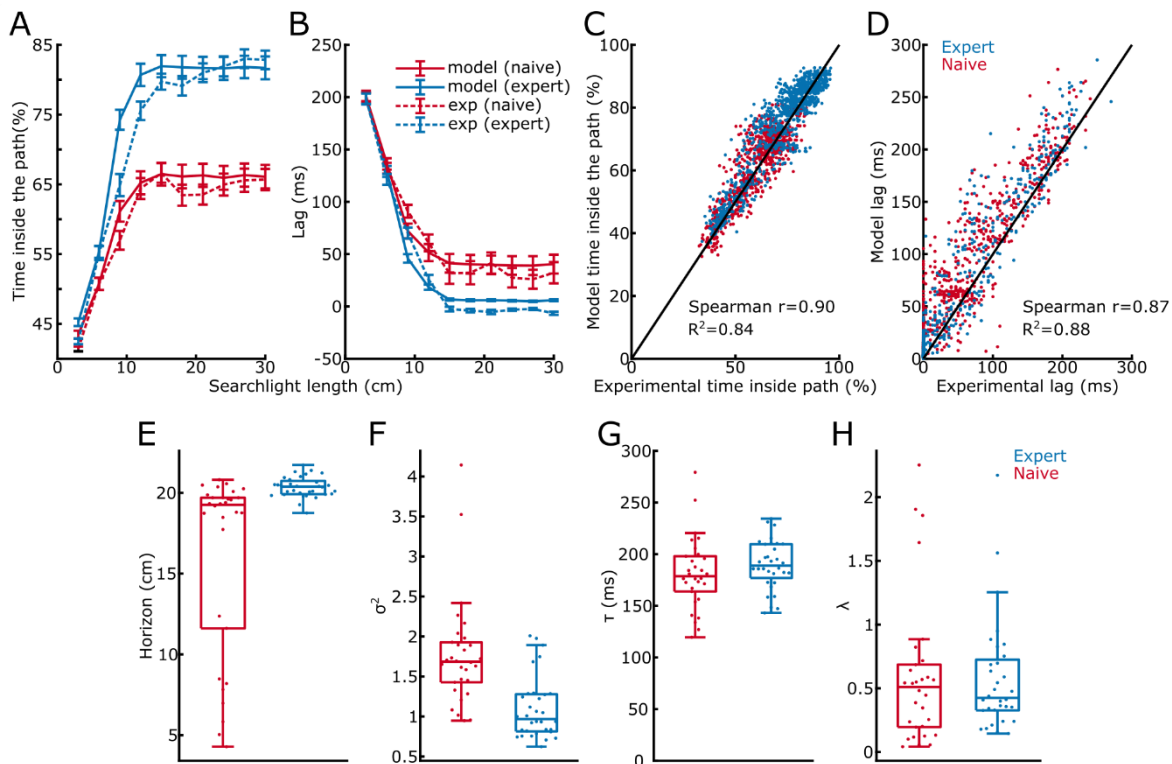
592 We compared the estimated model parameters between expert and naïve subjects. The fitted

593 model horizon was higher for the expert group than for the naïve group (Fig. 5E, Wilcoxon

594 ranksum test: $z=4.84$, $p=1\cdot 10^{-6}$, $N=62$) and was correlated with the horizon obtained from the

595 change point analysis (Spearman correlation, $r=0.48$, $p=7\cdot 10^{-5}$, $N=62$) and the exponential fits

596 (Spearman correlation, $r=0.43$, $p=6 \cdot 10^{-4}$, $N=62$). The fitted motor noise was significantly lower
 597 for the expert than for the naïve group (Fig. 5F; Wilcoxon ranksum test: $z=4.66$, $p=3 \cdot 10^{-6}$,
 598 $N=62$) while the delay and the penalty parameters were not different (Fig. 5G,H; delay:
 599 Wilcoxon rank sum test, $z=1.50$, $p=0.13$; penalty: Wilcoxon rank sum test, $z=0.528$, $p=0.60$,
 600 $N=62$). In the model, lower motor noise lead to steeper initial accuracy slope (Fig. 4C). The
 601 expert group having lower estimated motor noise hence agrees well with our observation that
 602 experts had steeper initial accuracy slope (Fig. 2F).
 603



604
 605 *Figure 5: Comparison between the receding horizon model and subjects' behaviour. A,B: Task*
 606 *performance and lag as a function of the searchlight for expert and naïve subjects for the*
 607 *experiments and model simulations. C,D: Scatter plot of model and experimental task*
 608 *performance and lag for each trial of each subject. E-H: Model parameters for the subjects*
 609 *from the naïve and the expert group. Each dot depicts one subject, boxplots show medians as*
 610 *well as first and third quartiles.*

611

612 Using the model fits obtained above, we estimated how much of the experts' gain in asymptote
613 performance was due to increased horizon vs. decreased noise. To do this, we simulate the
614 model with naive group parameters but expert group horizons (see Methods). This brings the
615 performance almost half-way to the expert performance (for large searchlights the performance
616 levelled off at 72% instead of 82% with lower horizon, compared to 66% for the naïve
617 subjects). We observe roughly the same increase (to 75%) when we simulate the model with
618 naive group parameters but expert group noise levels. Similarly, when we use expert group
619 parameters but naive group horizons or noise levels, the performance drops approximately half-
620 way to the naïve accuracy (74% for naïve horizon, 71% for naïve motor noise). In contrast, the
621 delay and the motor penalty parameters had less influence on the asymptote performance (63%
622 and 64% for naïve group parameters with expert delay or motor penalty; 80% for expert group
623 parameters with naïve delay or motor penalty). From this we conclude that the increase in the
624 experts' performance was caused by equal measures through an increase in planning horizon
625 and the decrease in motor noise.

626

627 **Discussion**

628

629 We used a paradigm that allowed us to study skill development when humans had to track an
630 unpredictable spatial path. The skill requires fast reactions to new upcoming bends in the road,
631 but also a substantial “planning ahead” component – i.e. the anticipation and preplanning of
632 movements that have to be made in the near future. We used the accuracy, i.e. the fraction of
633 time the cursor was inside the path boundaries, as the measure of performance. We observed a
634 substantial improvement in accuracy after 5 days of training (Fig. 1B,C). The paths were
635 different on every trial, so the improvement in performance cannot be attributed to a memory
636 for the sequence.

637

638 What changes in the motor system occur through learning that allowed skilled subjects to
639 perform better? We hypothesized that one important component is an increased ability to take
640 into account approaching path bends and to prepare for an upcoming movement segment. We
641 directly estimated subjects' planning horizons by using a searchlight testing where only a part
642 of the approaching curve was visible. We found that subjects with a higher tracking skill
643 demonstrated larger planning horizons: on average ~14cm for the expert group vs. ~11cm for
644 the naïve group, corresponding to the time horizons of ~0.4s and ~0.3s respectively.

645

646 Note that “planning”/“preparing” the movement can be interpreted differently depending on
647 the computational approach. In the framework of optimal control (Todorov and Jordan, 2002),
648 subjects do not plan the actual trajectory to be followed, but instead use an optimal time-
649 dependent feedback policy and then execute the movement according to this policy. The
650 observed increase in planning horizon can be interpreted in the framework of model predictive
651 control, also known as receding horizon control, RHC (Kwon and Han, 2005). In RHC, the

652 optimal control policy is computed for a finite and limited planning horizon, which may not
653 capture the whole duration of the trial. This policy is then applied for the next control step,
654 which is typically very short, and the planning horizon is then shifted one step forward to
655 compute a new policy. Hence, RHC does not use a pre-computed policy, optimal for an infinite
656 horizon, but a policy which is only optimal for the current planning horizon. Increasing the
657 length of the planning horizon is therefore likely to increase the accuracy of the control policy.
658 In our experiments this would allow for a larger fraction of time spent within the path
659 boundaries. We designed a simple RHC model to test directly which components in the model
660 would have to change through training to quantitatively explain the subject's behavior. The
661 dynamics of movement and the cost function were modelled in line with previous studies that
662 used optimal control to describe human behaviour in various motor control and learning tasks
663 (Todorov & Jordan 2002, Diedrichsen 2007, Braun et al. 2009). We fitted the RHC model to
664 the behaviour of each subject and found that it was able to fit the data very accurately (Fig. 5).
665 The experimentally observed differences between expert and naïve subjects were reflected in
666 the model fits by higher planning horizons and lower motor noise parameters in the expert
667 group. Our findings, thus, demonstrate that subjects' behaviour can be understood in the
668 context of RHC, and longer planning horizons of the expert group indicate that subjects learn
669 how to take advantage of future path information to improve motor performance.

670

671 The increased planning horizon does not account for all of the observed improvement in
672 performance and further motor and non-motor processes may play a role in tracking skill
673 learning. Indeed, our results show that expert subjects are even better at shorter searchlight
674 lengths, a phenomenon that is explained by the model in assuming better motor acuity (lower
675 motor noise) for expert subjects (Shmuelof et al., 2014, 2012). We estimated that in our
676 experiments nearly half of the increased performance after practice is due to an increased

677 planning horizon while the other half can be accounted for by a reduction in the motor noise
678 which may be interpreted as higher motor acuity.

679

680 **Related work**

681 Ideas similar to the RHC were put forward in a recent study (Ramkumar et al., 2016) that
682 suggested that movements are broken up in ‘chunks’ in order to deal with the computational
683 complexity of planning over long horizons. That study suggests that monkeys increase the
684 length of their movement chunks during extended motor learning over the course of many days
685 which may be explained by monkeys increasing their planning horizon with learning. At the
686 same time, the efficiency of movement control within the chunks improved with learning which
687 may also be the result of a longer horizon. Despite these potential consistencies with our
688 approach we note that in their model Ramkumar et al. (2016) assumed that ‘chunks’ are
689 separated by halting points (i.e. points of zero speed) and movements within ‘chunks’ are
690 optimized independently from each other. Our RHC model does not have independent
691 movement elements but movements are optimized continuously.

692

693 Even though our study, to the best of our knowledge, is the first to directly investigate the
694 evolution of the planning horizon during skill learning, similar path tracking tasks have been
695 used before (Poulton, 1974). Using a track that was drawn on a rotating paper roll, these early
696 studies found that the accuracy of the tracking increased with practice and with increasing
697 searchlight length (which was modified by physically occluding part of the paper roll, Poulton,
698 1974, p 187). These studies, however, did not investigate the effect of learning on the planning
699 horizon.

700

701 More recent studies used path tracking tasks where the goal was to move as fast as possible
702 while maintaining the accuracy (instead of moving at a fixed speed). In all of these studies the
703 identical path was repeatedly presented. In one study subjects had to track a fixed maze without
704 visual feedback and learnt to do it faster as the experiment progressed (Petersen et al., 1998);
705 there the subjects had to once “discover” and then remember the correct way through the maze.
706 In another series of experiments, Shmuelof et al. asked subjects to track two fixed semi-circular
707 paths. Subjects became faster and more accurate over the course of several days (Shmuelof et
708 al., 2012), but this increase in the speed and accuracy did not generalize to untrained paths
709 (Shmuelof et al., 2014). In contrast to these previous path tracking studies, we used randomly
710 generated paths throughout the experiment. By investigating the generalization of the path
711 tracking skill to novel paths we could reveal an increasing planning horizon with learning.

712

713 **Conclusion**

714 In conclusion, we have established that people are able to learn the skill of path tracking and
715 improve their skill over 5 days of training. This increase in motor skill is associated with the
716 increased planning horizon. The dynamics of preplanning can be well described by a receding
717 horizon control model.

718 **Acknowledgements**

719 The study was in parts supported by the German Federal Ministry of Education and Research
720 (BMBF) grant 01GQ0830 to BFNT Freiburg-Tübingen. The authors acknowledge support by
721 the state of Baden-Württemberg through bwHPC and the German Research Foundation (DFG)
722 through grant no INST 39/963-1 FUGG. The authors also thank the ‘Struktur- und
723 Innovationsfonds Baden-Württemberg (SI-BW)’ of the state of Baden-Württemberg for
724 funding.

725

726 **Author Contribution**

727 Conceptualization, LB. DK. and CM; Methodology, LB. DK. JD and CM; Formal Analysis,
728 LB. DK and CM; Writing – Original Draft, LB. DK and CM; Writing – Review and Editing,
729 LB, DK, JD and CM.

730

731 References

- 732 Bashford, L., Kobak, D., Mehring, C., 2015. Motor skill learning by increasing the movement planning horizon.
733 ArXiv14106049 Q-Bio.
- 734 Brainard, D.H., 1997. The Psychophysics Toolbox. *Spat. Vis.* 10, 433–436.
735 <https://doi.org/10.1163/156856897X00357>
- 736 Braun, D.A., Aertsen, A., Wolpert, D.M., Mehring, C., 2009. Learning Optimal Adaptation Strategies in
737 Unpredictable Motor Tasks. *J. Neurosci.* 29, 6472–6478. [https://doi.org/10.1523/JNEUROSCI.3075-](https://doi.org/10.1523/JNEUROSCI.3075-08.2009)
738 08.2009
- 739 Diedrichsen, J., 2007. Optimal task-dependent changes of bimanual feedback control and adaptation. *Curr. Biol.*
740 CB 17, 1675–1679. <https://doi.org/10.1016/j.cub.2007.08.051>
- 741 Diedrichsen, J., Kornysheva, K., 2015. Motor skill learning between selection and execution. *Trends Cogn. Sci.*
742 19, 227–233. <https://doi.org/10.1016/j.tics.2015.02.003>
- 743 Diedrichsen, J., Shadmehr, R., Ivry, R.B., 2010. The coordination of movement: optimal feedback control and
744 beyond. *Trends Cogn. Sci.* 14, 31–39. <https://doi.org/10.1016/j.tics.2009.11.004>
- 745 Dimitriou, M., Wolpert, D.M., Franklin, D.W., 2013. The Temporal Evolution of Feedback Gains Rapidly
746 Update to Task Demands. *J. Neurosci.* 33, 10898–10909. [https://doi.org/10.1523/JNEUROSCI.5669-](https://doi.org/10.1523/JNEUROSCI.5669-12.2013)
747 12.2013
- 748 Karni, A., Meyer, G., Jezzard, P., Adams, M.M., Turner, R., Ungerleider, L.G., 1995. Functional MRI evidence
749 for adult motor cortex plasticity during motor skill learning. *Nature* 377, 155–8.
750 <https://doi.org/10.1038/377155a0>
- 751 Karni, A., Meyer, G., Rey-Hipolito, C., Jezzard, P., Adams, M., Turner, R., Ungerleider, L., 1998. The
752 acquisition of skilled motor performance : Fast and slow experience-driven changes in primary motor
753 cortex. *Proc. Natl. Acad. Sci. U. S. A.* 95, 861–868.
- 754 Kwon, W.H., Han, S.H., 2005. *Receding Horizon Control: Model Predictive Control for State Models,*
755 *Advanced Textbooks in Control and Signal Processing.* Springer-Verlag, London.
- 756 Petersen, S.E., Mier, H. van, Fiez, J.A., Raichle, M.E., 1998. The effects of practice on the functional anatomy
757 of task performance. *Proc. Natl. Acad. Sci.* 95, 853–860.
- 758 Poulton, E.C., 1974. *Tracking Skill and Manual Control.* Academic Press, Incorporated, New York, N.Y.
- 759 Ramkumar, P., Acuna, D.E., Berniker, M., Grafton, S.T., Turner, R.S., Kording, K.P., 2016. Chunking as the
760 result of an efficiency computation trade-off. *Nat. Commun.* 7, 12176.
761 <https://doi.org/10.1038/ncomms12176>
- 762 Shadmehr, R., Smith, M.A., Krakauer, J.W., 2010. Error Correction, Sensory Prediction, and Adaptation in
763 Motor Control. *Annu. Rev. Neurosci.* 33, 89–108. [https://doi.org/10.1146/annurev-neuro-060909-](https://doi.org/10.1146/annurev-neuro-060909-153135)
764 153135
- 765 Shmuelof, L., Krakauer, J.W., Mazzoni, P., 2012. How is a motor skill learned? Change and invariance at the
766 levels of task success and trajectory control. *J. Neurophysiol.* 578–594.
767 <https://doi.org/10.1152/jn.00856.2011>
- 768 Shmuelof, L., Yang, J., Caffo, B., Mazzoni, P., Krakauer, J.W., 2014. The neural correlates of learned motor
769 acuity. *J. Neurophysiol.* 112, 971–980. <https://doi.org/10.1152/jn.00897.2013>
- 770 Todorov, E., Jordan, M.I., 2002. Optimal feedback control as a theory of motor coordination. *Nat. Neurosci.* 5,
771 1226–1235. <https://doi.org/10.1038/nn963>
- 772 Walker, M.P., Brakefield, T., Morgan, A., Hobson, J.A., Stickgold, R., 2002. Practice with Sleep Makes
773 Perfect : Sleep-Dependent Motor Skill Learning. *Neuron* 35, 205–211.
- 774 Waters-Metenier, S., Husain, M., Wiestler, T., Diedrichsen, J., 2014. Bihemispheric Transcranial Direct Current
775 Stimulation Enhances Effector-Independent Representations of Motor Synergy and Sequence Learning.
776 *J. Neurosci.* 34, 1037–1050. <https://doi.org/10.1523/JNEUROSCI.2282-13.2014>
- 777 Wolpert, D.M., Diedrichsen, J., Flanagan, J.R., 2011. Principles of sensorimotor learning. *Nat. Rev. Neurosci.*
778 12, 739–51. <https://doi.org/10.1038/nrn3112>
- 779 Wong, A.L., Lindquist, M.A., Haith, A.M., Krakauer, J.W., 2015. Explicit knowledge enhances motor vigor and
780 performance: motivation versus practice in sequence tasks. *J. Neurophysiol.* 114, 219–232.
781 <https://doi.org/10.1152/jn.00218.2015>
- 782
- 783